Supporting Information

for

Photoinitiated Singlet and Triplet Electron Transfer Across a Re-Designed [Myoglobin, Cytochrome b_5] Interface

Judith M. Nocek,[†] *Amanda K. Knutson,*[†] *Peng Xiong,*

*Nadia Petlakh Co, and Brian M. Hoffman**

Department of Chemistry, Northwestern University,

2145 Sheridan Road, Tech K148, Evanston, IL 60208

[†]These authors contributed equally to this manuscript.

*Corresponding author.

MATERIALS AND METHODS

Expression and Purification of Cytochrome b_5

The plasmid for the 82-residue fragment of $Fe^{3+}b_5$ was obtained from Professor A. Grant Mauk. Cultures of *E.coli* containing this plasmid were grown, cells were isolated, and $Fe^{3+}b_5$ was extracted and purified as described previously.[1]

Mb and Mb Mutants

Construction of Mb Mutants: The Mb(D44K), Mb(D60K), and Mb(E85K) single mutants and the Mb(D44K/D60K) double mutant, Mb(+4), were constructed using the method of overlap extension. Four primers are required for each mutation. Two of them flank sequences on the horse heart Mb(WT) plasmid, pGYM: the RV-M primer, 5'- GAG CGG ATA ACA ATT TCA CAC AGG -3' and the M13-47 primer, 5'- CGC CAG GGT TTT CCC AGT CAC GAC-3'. The other two primers contain the mutation sites (**Table S1**), where the codon that determines the mutation site is underlined. DNA fragment 1 containing the mutation site and upstream sequences was amplified using the RV-M primer, the reverse primer containing the mutation site and the Mb(WT) plasmid (pGYM) as a template; DNA fragment 2 containing the mutation site and downstream sequences was amplified using the M13-47 primer and the forward primer containing the mutation site and pGYM as a template. Finally, the full-length Mb DNA was amplified with RV-M and M13-47 as primers and the mixture of DNA fragment 1 and fragment 2 as a template. This full-length mutated Mb DNA was digested with PstI and BamHI, and the PstI/BamHI fragment was inserted back into the same restriction sites of the Mb(WT) plasmid.[2]

The plasmid for the Mb(D44K/D60K/E85K) triple mutant (Mb(+6)) was constructed with a QuikChange mutagenesis kit using the Mb(+4) plasmid as a template, the 5'- A GGG CAC CAC GAA GCT AAG CTC AAA CCG C - 3' oligomer as forward primer and the 5'- G

CGG TTT GAG CTT AGC TTC GTG GTG CCC T - 3' oligomer as reverse primer. The sequences of all the mutated plasmids were verified by DNA sequencing (SeqWright).

Table S1: Primers for preparation of single and multiple mutants

Mb	Forward Primer	Reverse Primer
D44K	5'- G GAA AAA TTC AAG AAA TTC AAA C - 3'	5'- G TTT GAA TTT CTT GAA TTT TTC C - 3'
D60K	5'-G GCG TCT GAA AAG CTG AAA AAA CAT G-3'	5'-C ATG TTT TTT CAG CTT TTC AGA CGC C-3'
E85K	5'- A GGG CAC CAC GAA GCT AAG CTC AAA CCG C - 3'	5'- G CGG TTT GAG CTT AGC TTC GTG GTG CCC T - 3'

Expression and Purification of Mb and Mb Mutants: The Mb mutants were over-expressed in *E.coli*, isolated and purified according to the procedures described previously for Mb(WT).[3] Briefly, the plasmids were transformed into *E.coli* BL21(DE3) cells, and grown at 37°C overnight on LB plates. A single colony was selected and used to inoculate 100 ml portions of LB. After incubation for 3 hrs, this culture was used to inoculate six larger batches of growth media (2 L of LB media in 4 L flasks) which were incubated at 37^0 C for 20 hrs.

Dark red cells containing oxyMb were harvested by centrifugation, collected, and resuspended in cold Tris/HCl (20 mM, pH 8.0). The resulting cell suspension was digested with lysozyme (Sigma) at 4°C until the cells turned viscous (~2 hrs). Next, deoxyribonuclease I (Sigma), ribonuclease A (Sigma) and $MgCl_2$ were added and the cells were stirred at 4^0C for an additional 3 - 4 hrs until the solution was no longer viscous. Cell debris was removed by centrifugation (Sorvall GS3 rotor, 8500 rpm, 40 min) and the supernatant was collected. The pellet was washed with cold 20 mM Tris/HCl pH 8.0 and the centrifugation step was repeated to ensure recovery of all protein.

The red supernatant was slowly brought to 65% saturation with solid $(NH_4)_2SO_4$ and the proteins precipitated for 3 hrs on ice. Following centrifugation, the supernatant liquid was slowly

brought to 95% saturation with solid $(NH_4)_2SO_4$. The solution was stored on ice overnight. The precipitate collected by centrifugation was resuspended in a minimal amount of water and dialyzed against 5 mM Tris/HCl buffer (pH 8.4). The sample was then applied to a DEAE-CL6B column (4.5 x18 cm) which had been equilibrated with 5 mM Tris/HCl, pH 8.4 at 4˚C, and the protein was eluted with a flow rate of 1mL/min using a linear gradient consisting of 500 ml buffer A (5 mM Tris/HCl, pH 8.4) and 500 ml buffer B (5 mM Tris/HCl, pH 8.4, 0.15 M NaCl). Fractions were assayed for purity on 20% SDS-PAGE. Fractions containing metMb were pooled and concentrated by ultrafiltration (Amicon Centriprep-3) for loading onto a G-75 column pre-equilibrated with buffer C (20 mM Tris/HCl pH 8.4). The final purity of the protein was assessed by UV-vis spectroscopy A_{410}/A_{280} and SDS-PAGE.

As the yields for the Mb(+4) and Mb(+6) are noticeably lower, several modifications to the procedures for growth and expression were implemented. First, we inserted a third stage in the growth procedure. A single colony was selected and used to inoculate 2 ml of LB medium containing 200 μg/l ampicillin. Aliquots of this primary culture (100 μl) were used to inoculate 50 ml portions of media, and 4 ml aliquots from these intermediate size cultures were used to inoculate the larger 2L batches. The growth times were optimized during each stage such that incubation proceeded until $OD_{600\ nm}$ reached 0.3-0.5 (first stage), 0.5 (second stage) and 0.5-0.8 (final stage). In the last stage, the shaking speed was lowered from 200 rpm to 125 rpm. As this inevitably increased the overall growth time required for the cultures to reach completion, we added an additional aliquot of ampicillin to reduce the chances for contamination. Further, we added freshly-prepared $FeSO_4$ solution (100 μg/L) in this final stage to enhance heme synthesis.

The increased charge of Mb(+6) also required modifications in the purification process. Since both the charge and size of lysozyme are similar to that of Mb(+6), the cells were lysed by

sonication to avoid interference from lysozyme during purification. As Mb(+6) bound too tightly to an anion exchange resin, CM-52 cation exchange resin (Whatman) was used instead. For this column, the protein was loaded in 10 mM KPi (pH7) and eluted with a high salt buffer (10 mM KPi at pH7, with 0.1 M KCl).

Preparation of and Characterization of ZnDMbs: ApoMb was prepared using the acid-butanone extraction method[4] and reconstituted with Zn-deuteroporphyrin IX (ZnD, Frontier Scientific) according to published procedures.[5-7] Excess heme was separated from the reconstitution mixture on a Sephadex G25-50 size exclusion column.

Molecular weights were measured in the IMSERC Facility at NU by electrospray ionization mass spectrometry (Agilent 6210 LC-TOF). Samples were desalted and concentrated to ~ 0.2 mM. The ion profile for the recombinant Mb(WT) shows two components, as reported by Mauk, et al.[8] The mass of the minor component (16,950 D) matches the expected mass for Mb(WT), while the mass of the major component (17,082 D) corresponds to a form of apo-Mb(horse) with an additional Met at its N–terminus. Consistent with this, we find that the higher mass component is not observed in native Mb. As the Mb mutants derive from this construct, they likewise show two components.

To remove the heavier component, samples were incubated overnight at 37°C with $5x10^{-3}$ units of methionine aminopeptidase (*Pyrococcus furiosus*, recombinant, Sigma) and 0.2 mM $CoCl_2$, 50 mM KPi at pH 7.5.[9] Samples were assayed by mass spectroscopy before and after incubation to insure that the reaction was complete. The component that remains after treatment of either the Fe^{3+}Mb or ZnMb derivatives of the mutants with methionine aminopeptidase show the expected mass increases: Mb(+4) shows an increase in mass of +27 D relative to Mb(WT);

Mb(+6) shows an increase in mass of +25 D relative to Mb(WT). All kinetics measurements were performed without regard to the presence of the additional methionine.

The thermal stability of the mutants was tested using CD spectroscopy. Samples (2 μM) were prepared in working buffer (10 mM KPi, pH7) under nitrogen and spectra were collected in the Keck Biophysics Facility with a Jasco J-715 spectrometer. Each spectrum was recorded from 190-450 nm at a scan speed of 100 nm/min, a response time of 2 s, and a bandwidth of 1 nm, averaged over 5 scans. In the thermal denaturation experiments, the ellipticity at 220 nm was monitored while the temperature was ramped from 20^{o}C to 80^{o}C in 2°/min intervals.

Binding and Kinetics

Sample Preparation: Protein stock solutions were exchanged into working buffer prior to the experiment using Centricon 10 microconcentrators. Samples for triplet quenching experiments (~5 μM ZnMb) were prepared in the dark under a nitrogen atmosphere as described previously.[7] Oxy-Mb and carboxy-Mb for ligand rebinding measurements were prepared by reducing met-Mb with a slight excess of sodium dithionite under a blanket of either O_2 or CO. Excess reductant was then removed by passing the sample through a size-exclusion column. An aliquot of the stock solution was transferred to a CO/O_2-saturated buffer ([O_2] = [CO] = 1 mM at ambient[10] with an air-tight syringe. Concentrations of stock solutions were determined spectrophotometrically with a diode array spectrophotometer (Agilent 8453): ZnDMbs, $\varepsilon_{414\ nm}$ = 364.1 $mM^{-1}cm^{-1}$;[11] $Fe^{3+}b_5$, $\varepsilon_{413\ nm}$ = 117 $mM^{-1}cm^{-1}$;[12] MbO_2, $\varepsilon_{418\ nm}$ = 133 $mM^{-1}cm^{-1}$;[13] MbCO, $\varepsilon_{424\ nm}$ = 207 $mM^{-1}cm^{-1}$.[13]

Flash Photolysis: Triplet quenching and ligand rebinding measurements were performed with an LKS.60 laser flash photolysis spectrometer (Applied Photophysics) equipped with a Xe-arc lamp that could be pulsed for short time measurements (20 ns - 5 μs). The 'fast' collection

mode uses an Agilent Infiniium 600 MHz digitizer with a 5-stage photomultiplier tube as detector; the 'slow' configuration uses a modified stopped-flow setup (Applied Photophysics, SX20) for digitization with a 9-stage photomultiplier tube. Reactions were initiated using the frequency-doubled output of a Nd:YAG pulsed laser (Spectra-Physics INDI 40-10-HG) operating at 10 Hz. The laser power density was adjusted to achieve quantitative conversion to the singlet state, so that excited state populations would reliably reflect the ground state equilibrium populations. As decay traces may span up to 6 orders of magnitude in time, we collected data in segments on short and long timescales. Short timescales are averages of 100 shots; long timescales are averages of 20 shots. These were merged into a single file to obtain full progress curves for analysis. Timecourses for the triplet state were collected at 475 nm, a maximum in the triplet-ground difference spectrum. Timecourses for O_2-rebinding were collected at 450 nm. All kinetic experiments were performed at 20^{o}C.

Decays of the first excited triplet state determined from the time-resolved transient absorption signals collected near the absorbance maximum in the ^{3}Zn-Zn difference spectrum (475 nm) are well-described by an exponential function: k_D(Mb(+4)) = 110(±15) s^{-1} and k_D(Mb(+6)) = 135(± 65) s^{-1}, k_D(Mb(WT)) = 50(± 5) s^{-1}.[5,6,14] The relative invariance of k_D and of the absorption spectra of both the Zn- and Fe^{3+}Mbs shows that the heme environment is not perturbed by these mutations. This is of particular note, as the crystal structure of Fe^{3+}Mb(horse)[15] shows that the Lys 45 residue adjacent to one of the mutation sites is hydrogen-bonded to the carboxylate of the heme 7-propionate.

Binding Measurements: Binding curves were analyzed using the isotherm of **Eq 1** where K_d is the dissociation constant, D_0 is the initial concentration of the ZnDMb donor, and A_0 is the concentration of its Fe^{3+}*b*$_5$ ET partner, which increases during a titration:

$$f(A_0) = [K_d + D_0 + A_0 - ((K_d + D_0 + A_0)^2 - 4\, D_0\, A_0)^{1/2}\ ] / (2\, D_0) \qquad \textbf{(1)}$$

The fraction of ZnDMb bound in a [Mb, $Fe^{3+}b_5$] complex (*f*) is obtained from quenching experiments as described in the text (**Eq 7, 9**).

Computations

Electrostatic Properties: Electrostatic properties were computed using a Linux version of the MacroDox program[16] as previously described.[5] The starting structures for these computations were the x-ray coordinates of Fe^{3+}Mb (1ymb.pdb)[15] and the tryptic fragment of $Fe^{3+}b_5$ (1cyo.pdb).[17] Coordinates for all crystallographically identified solvent molecules and ions were deleted. When the structure file included multiple conformations, only the coordinates for conformer A were used and no effort was made to compare results to those obtained with the alternate configurations. Mutant structures were built from the coordinates for the parent and the protonation states of the titratable residues were assigned using the Tanford-Kirkwood calculation with the static accessibility modification using atom parameters obtained with the CHARMM force field. Each residue was assigned a net charge based on its environment, pH, ionic strength, and temperature (unless otherwise noted, pH 7, μ =18 mM, T = 20^{o}C) with the assumptions that: *i*) all Lys residues are fully protonated; *ii*) all Arg and all His (except for the protein ligands) are fully protonated with the charge partitioned between the two nitrogen atoms; *iii*) the carboxylate groups of the Asp and Glu residues and the heme propionates are fully deprotonated with the charge partitioned between the two carboxylate oxygen atoms; *iv*) the ligands of $Fe^{3+}b_5$ (H39 and H63) and Fe^{2+}Mb (H93) were uncharged; *v*) a formal charge of '0' was assigned to Fe^{2+} of Mb and a formal charge of +1 was assigned to $Fe^{3+}$of b_5.

Brownian Dynamics Docking Calculations: In the present study, we considered two different reaction distance criteria: *i*) center-of-mass criterion (COM) in which a successful hit occurs when the distance between the center-of-mass of the two proteins are within 39 Å, approximately the sum of the radii of the partner proteins; *ii*) propionate contact criterion (O-O) in which a hit occurs if any heme propionate oxygen atom on one protein is within 4.0 Å of a heme propionate oxygen atom of its partner. Hits derived using the O-O criterion represent ET-active configurations and are useful for examining effects on reactive binding, while hits derived using the COM criterion include all configurations with the partners in close contact and are useful for probing overall binding. To obtain satisfactory statistical results, we found it necessary to use no fewer than 10,000 trajectories.

HyPARE Calculations: The HyPARE program[18] developed by Schreiber and coworkers (http://bioportal.weizmann.ac.il/hypareb/main.) was used to calculate the enhancements in the association rate constants of a [Mb, b_5] complex due to mutation of each residue to either a positively-charged, negatively-charged or neutral residue. The hot spot maps we report here show relative association enhancements and are independent of the input values for the experimental ionic strength and association rate constant.

Characterization of Mb Surface Mutants

To experimentally test the predictions arrived at from BD simulations, we prepared the Mb(+4) and Mb(+6) mutants in their ferriheme forms, and to enable the study of photoinitiated ET with $Fe^{3+}b_5$, we incorporated Zn-deuteroporphyrin (ZnD) into each of the Mb variants. The resulting proteins were characterized by a variety of techniques.

Circular Dichroism Spectra: CD spectra for the Zn-substituted derivatives of Mb(WT), and the two mutants are given in **Fig S1**. At 20°C all three proteins show negative ellipticities (θ) at 208 nm and 222 nm that are characteristic of α-helices.[19] The spectra of the two mutants are essentially identical to that of Mb(WT),[20] indicating that they are properly folded. Measurements made during progressive heating (**Fig S1, inset**) show that the onset of denaturation for the ZnDMb(WT) does not begin until ~ 80°C, whereas the onset for the mutants occurs at ~ 60°C. As all ET experiments were performed at a temperature of 20°C, we may assign the results to protein in the native, fully folded configuration. Additional spectra taken at 80°C show a greater decrease in ellipticity of the mutants than the Mb(WT), indicative of lower stability at elevated temperatures.

Ligand–Rebinding to Fe(II)Mb: We used flash photolysis/ligand-recombination to measure the rebinding kinetics for $(Fe^{2+}L)$Mb (**Fig S2)** for WT and mutant Mb, to test for possible localized perturbations in the heme pocket by charge changes in the vicinity. Recombination with CO at ambient temperatures is pseudo-first-order, with second-order rebinding rate constants of k_{CO} = 660 s^{-1} (WT), consistent with the previously reported value,[21] and k_{CO} = 680 s^{-1} (Mb(+4)). As expected, no geminate rebinding phase is observed at this temperature.

As a better probe of the flexibility of the Mb heme pocket, we examined the O_2-rebinding kinetics of the Fe^{2+}Mbs, which exhibits a unimolecular geminate phase along with the slower, bimolecular recombination phase.[22] The geminate recombination could be described for this purpose as the sum of two stretched exponentials, the bimolecular phase rate by a single pseudo-first-order phase. Within error, the traces for WT and mutants were the same. The two ligand binding experiments, thus indicate that the structure and dynamics of the heme pocket are essentially unperturbed by the mutations.

Absorption/Emission and Triplet-State Decay: The optical spectra of WT and mutant ferri-Mbs are indistinguishable. Likewise, spectra of the ZnD-porphyrin substituted Mb mutants are identical to those reported previously for ZnDMb(WT): λ_{max} = 414 nm, 542 nm and 580 nm.[23] The steady-state luminescence spectra of both mutants are identical to that of ZnDMb(WT) with peaks at 583 nm (2.12 eV) and 640 nm (1.94eV) attributed to $S_1[0] \rightarrow S_0[0]$ and $S_1[0] \rightarrow S_0[1]$ fluorescence. The peak maxima are similar to those published for zinc mesoporphyrin Mb.[24]

Discussion of Fig S6

An alternative, more detailed presentation of the progressive change in docked structures with increased Mb front-face positive charge is obtained by following the changes in the frequency with which a specific residue on Mb or $Fe^{3+}b_5$ appears among the ten shortest interfacial contacts for the ensemble of BD hit configurations. This is displayed in the histograms in **Fig S6**, which include both charged and uncharged residues (in contrast to earlier work [7,23,25]) so that repulsive and attractive electrostatic interactions, as well as van der Waals interactions between uncharged residues, are identified. These histograms show that no residue makes a short contact in a high percentage of hits for the [Mb(WT), $Fe^{3+}b_5$] complex, but that several residues do so for the mutants. Interestingly, the residues that appear in the interfaces are different for the two mutant complexes, suggesting that the average structures of these complexes are different.

On the $Fe^{3+}b_5$-side of the interface, four residues of $Fe^{3+}b_5$ make frequent contact with both of the Mb mutants (E48, E56, D60 and T88) and one additional residue (E44) makes frequent contact with Mb(+6). The set of frequent contacts does not include the heme of $Fe^{3+}b_5$, for these contacts likely require facilitating events that would neutralize the heme-heme repulsion, such as transient protonation of one of the heme carboxylates and/or formation of water bridges that are not included in the simulations. Bigger differences occur on the Mb-side of the interface where in addition to residue K63 and the Mb heme which are frequent contacts in the interfaces of both mutant complexes, residues K45 and K96 stabilize the Mb(+4) complex and residues K45, T70, K78, as well as the E85K mutation site stabilize Mb(+6) complex. Overall, the two representations of the BD results provided by **Figs 9, S6** provide revealing insights into how increasing the Mb front-face positive charge with two and then three charge-

reversal mutations progressively generates a more tightly-defined ensemble of structures for the [Mb, $Fe^{3+}b_5$] complex.

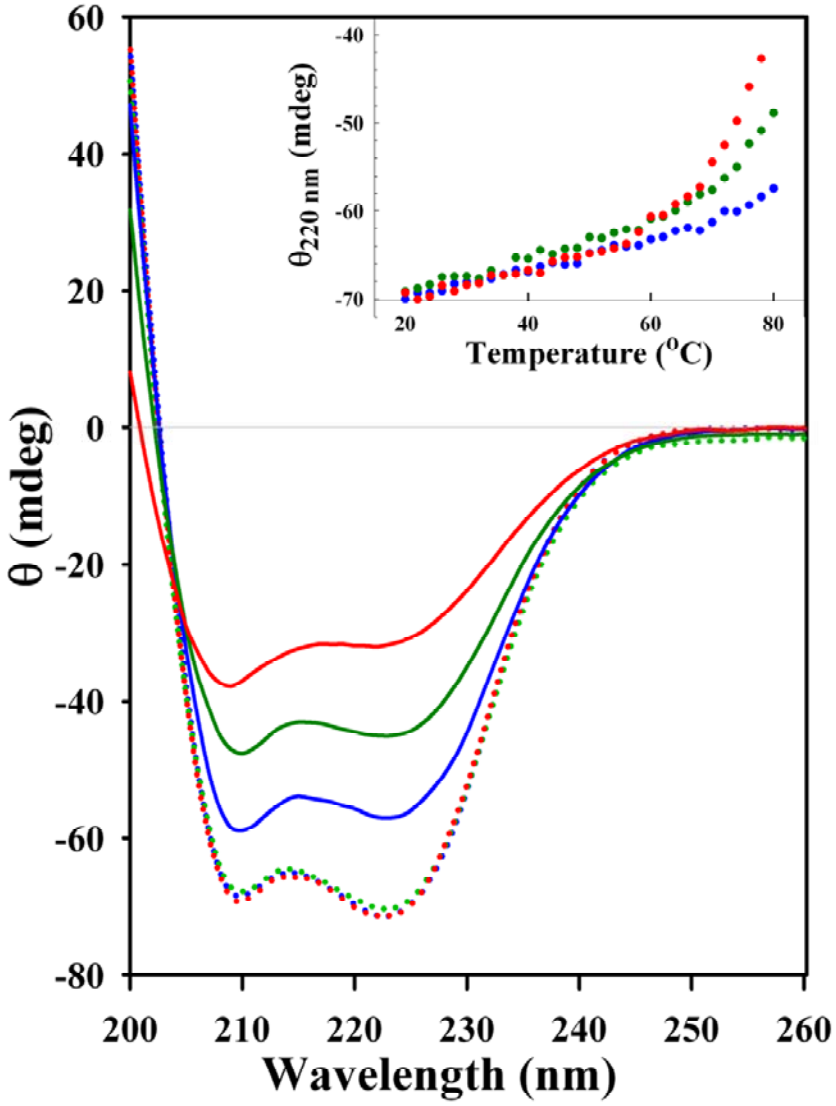

Fig S1:CD spectra for ZnMb(WT) (blue), ZnMb(+4) (green) and ZnMb(+6) (red). *Conditions*: 10mM KPi buffer, pH 7, [Mb] = 2 μM. Solid lines refer to spectra at 80°C; dotted lines refer to traces at 20°C. Thermal denaturation profiles are shown in the inset.

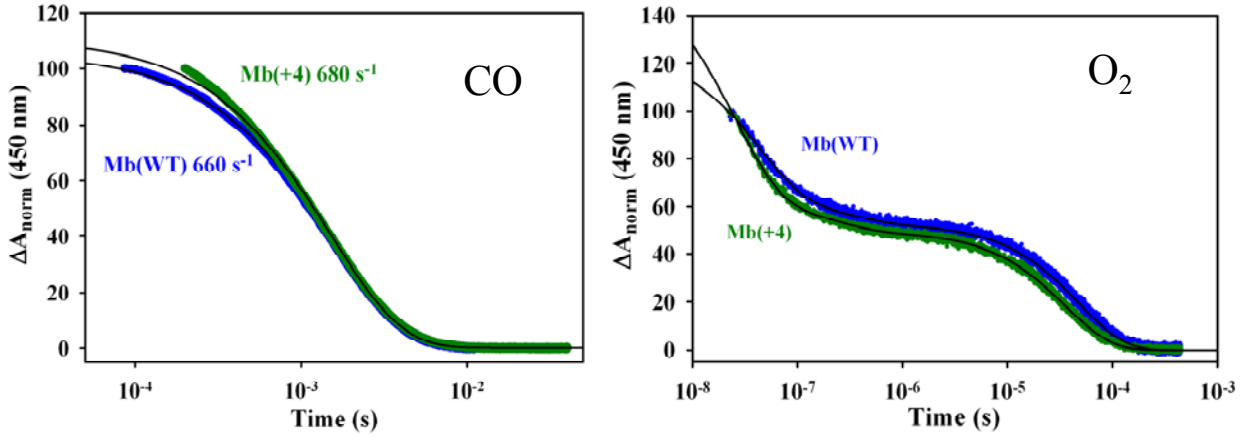

Fig S2:CO- (left) and O_2- rebinding (right) to Mb(WT) (blue) and Mb(+4) (green). *Conditions*: 10 mM KPi buffer, pH 7.

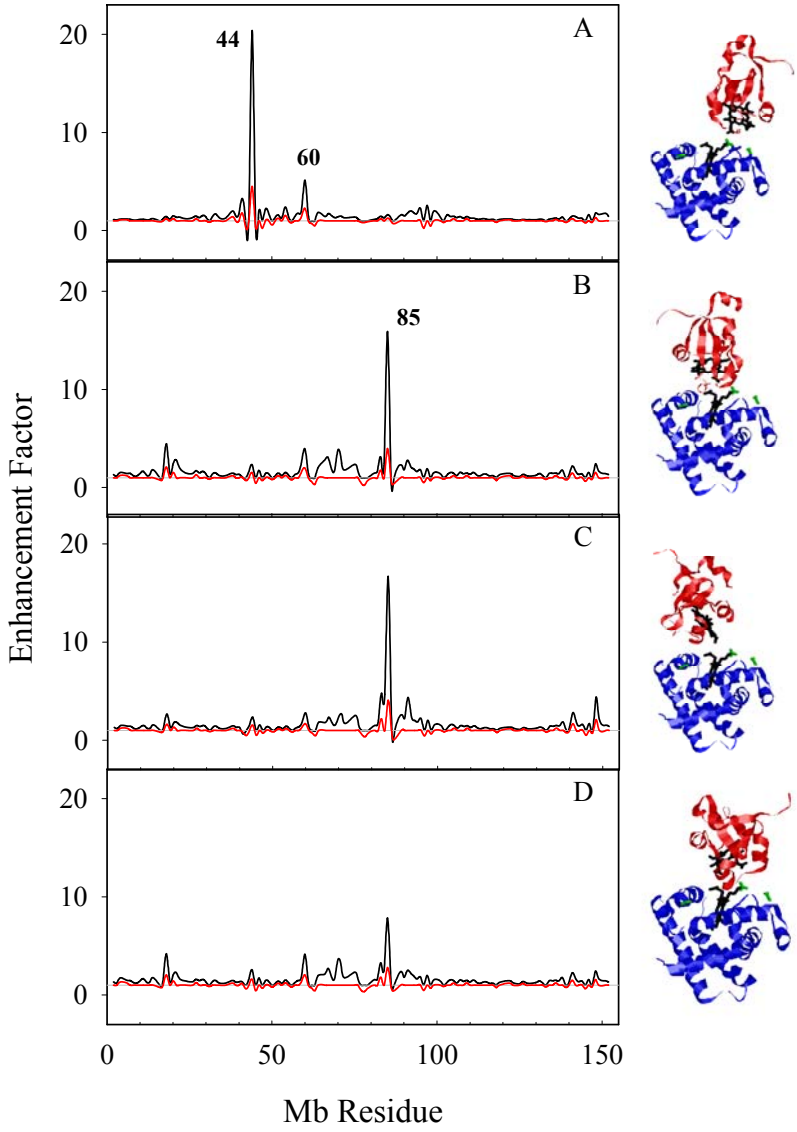

Fig S3:Relative enhancements in the association rate constants determined with HyPARE[18]as a function of sequence position. The four short O-O configurations obtained from a COM Brownian dynamics simulation with Mb(WT) were used as input structures. Results for replacements with a positively charged residue (k_+) are shown in black; results for Ala substitutions (k_{Ala}) are shown in red.

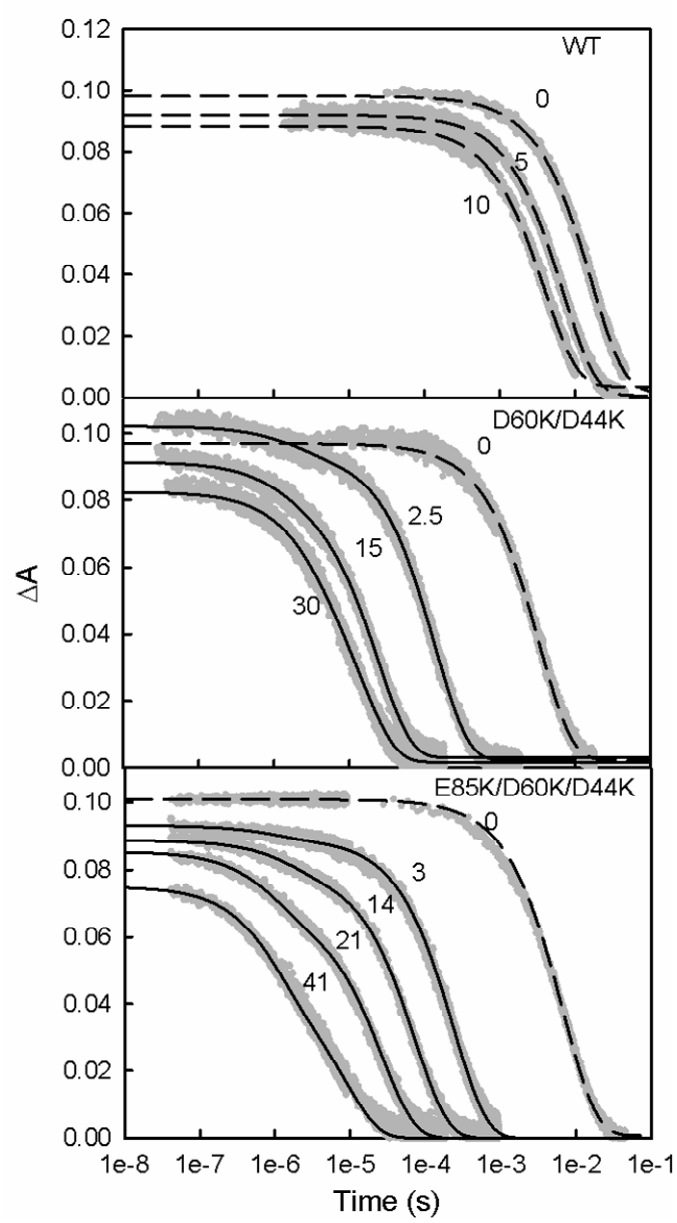

Fig S4:Triplet decay traces during titrations of ZnMb(WT), ZnMb(+4), and ZnMb(+6) with $Fe^{3+}b_5$. *Conditions*: 10 mM KPi buffer; pH 7; [ZnMb] = 5 μM. Numbers indicate the concentration of quencher in μM.

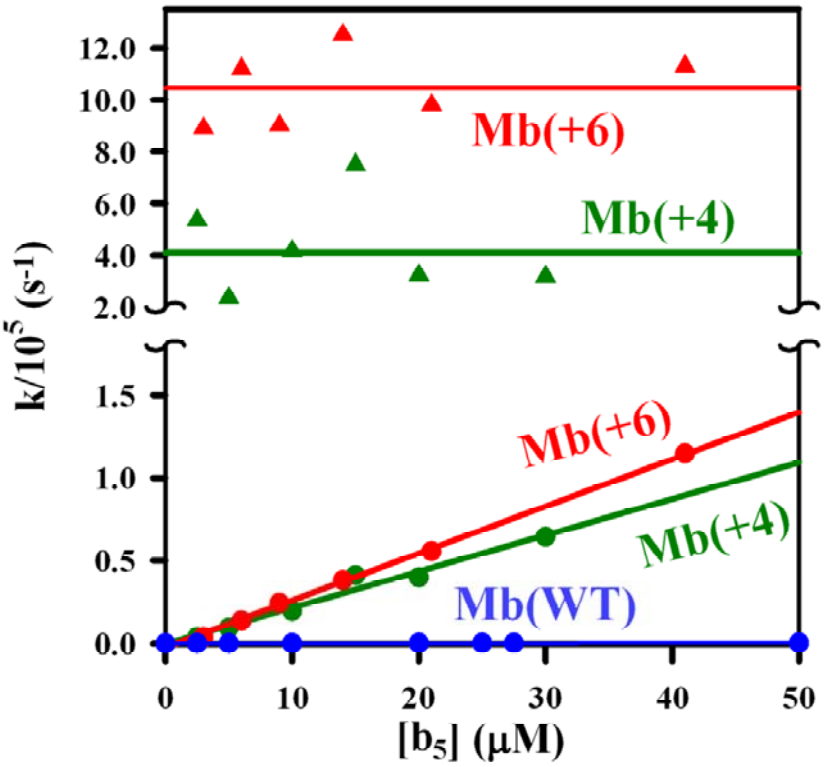

Fig S5:The bimolecular quenching rate constants from the slow phase (k_2) and the unimolecular rate constants from the fast phases (k_1) during titrations of ZnMb(+6), ZnMb(+4) and ZnMb(WT) with $Fe^{3+}b_5$. Data from **Fig S4**.

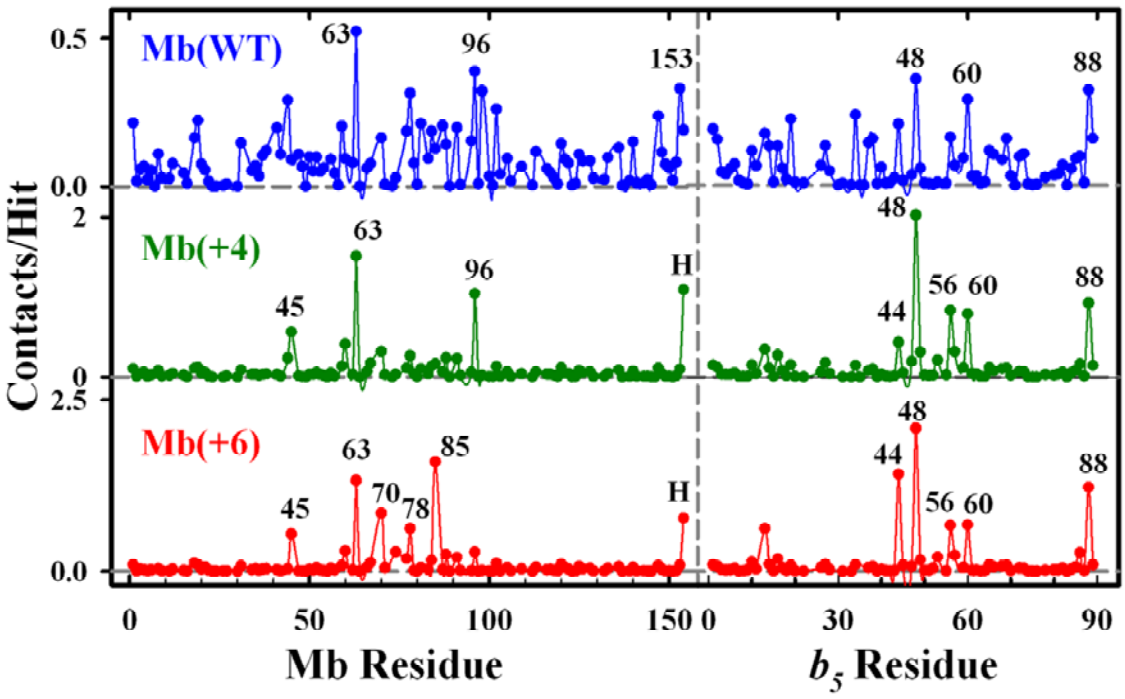

Fig S6:Contact frequency as a function of sequence position from COM simulations for docking of $Fe^{3+}b_5$ onto Mb(WT) (blue), Mb(+4) (green) or Mb(+6) (red). Conditions: μ = 18 mM, pH =7, T= 293K.

References

(1) Reid, L. S.; Mauk, M. R.; Mauk, A. G. *J. Am. Chem. Soc.* **1984**, *106*, 2182-2185.

(2) Guillemette, J. G.; Matsushima-Hibiya, Y.; Atkinson, T.; Smith, M. *Protein Eng.* **1991**, *4*, 585-592.

(3) Funk, W. D.; Lo, T. P.; Mauk, M. R.; Brayer, G. D.; MacGillivray, R. T. A.; Mauk, A. G. *Biochemistry* **1990**, *29*, 5500-5508.

(4) Teale, F. W. J. *Biochim. Biophys. Acta* **1959**, *35*, 543.

(5) Wheeler, K. E.; Nocek, J.; Cull, D. A.; Yatsunyk, L. A.; Rosenzweig, A. C.; Hoffman, B. M. *J. Am. Chem. Soc.* **2007**, *129*, 3906-3917.

(6) Liang, Z.-X.; Kurnikov, I. V.; Nocek, J. M.; Mauk, A. G.; Beratan, D. N.; Hoffman, B. M. *J. Am. Chem. Soc.* **2004**, *126*, 2785-2798.

(7) Nocek, J. M.; Sishta, B. P.; Cameron, J. C.; Mauk, A. G.; Hoffman, B. M. *J. Am. Chem. Soc.* **1997**, *119*, 2146-2155.

(8) Lloyd, E.; Mauk, A. G. *FEBS Lett.* **1994**, *340*, 281-286.

(9) Ben-Bassat, A.; Bauer, K.; Chang, S. Y.; Myambo, K.; Boosman, A.; Chang, S. *J. Bacteriol.* **1987**, *169*, 751-757.

(10) Weast, R. C.; Editor *Handbook of Chemistry and Physics. 58th Ed*, 1977.

(11) Wheeler, K. E.; Lees, N. S.; Gurbiel, R. J.; Hatch, S. L.; Nocek, J. M.; Hoffman, B. M. *J. Am. Chem. Soc.* **2004**, *126*, 13459-13463.

(12) Ozols, J.; Strittmatter, P. *J. Biol. Chem* **1964**, *239*, 1018-1023.

(13) Antonini, E.; Brunori, M. *Hemoglobin and Myoglobin in Their Reactions with Ligands*; North Holland Publishing Co.: Amsterdam, 1971.

(14) Nocek, J. M.; Zhou, J. S.; Hoffman, B. M. *J. Electroanal. Chem.* **1997**, *438*, 55-60.

(15) Evans, S. V.; Brayer, G. D. *J. Mol. Biol.* **1990**, *213*, 885-897.

(16) Northrup, S. H.; Thomasson, K. A.; Miller, C. M.; Barker, P. D.; Eltis, L. D.; Guillemette, J. G.; Inglis, S. C.; Mauk, A. G. *Biochemistry* **1993**, *32*, 6613-6623.

(17) Durley, R. C. E.; Mathews, F. S. *Acta Crystallographica* **1996**, *D52*, 65-76.

(18) Shaul, Y.; Schreiber, G. *Proteins: Struct., Funct., Bioinf.* **2005**, *60*, 341-352.

(19) Kelly, S. M.; Price, N. C. *Curr. Protein Pept. Sci.* **2000**, *1*, 349-384.

(20) Holzwarth, G.; Doty, P. *J. Am. Chem. Soc.* **1965**, *87*, 218-228.

(21) Nienhaus, K.; Deng, P.; Kriegl, J. M.; Nienhaus, G. U. *Biochemistry* **2003**, *42*, 9647-9658.

(22) Olson, J. S.; Soman, J.; Phillips, G. N., Jr. *IUBMB Life* **2007**, *59*, 552-562.

(23) Liang, Z.-X.; Nocek, J.; Huang, K.; Hayes, R. T.; Kurnikov, I. V.; Beratan, D. N.; Hoffman, B. M. *J. Am. Chem. Soc.* **2002**, *124*, 6849-6859.

(24) Hayashi, T.; Takimura, T.; Ogoshi, H. *J. Am. Chem. Soc.* **1995**, *117*, 11606-11607.

(25) Liang, Z.-X.; Jiang, M.; Ning, Q.; Hoffman, B. M. *JBIC* **2002**, *7*, 580-588.